HHS Public Access

Author manuscript

Clin Cancer Res. Author manuscript; available in PMC 2015 June 04.

Published in final edited form as:

Clin Cancer Res. 2012 September 1; 18(17): 4669–4681. doi:10.1158/1078-0432.CCR-12-0779.

Dual inhibition of canonical and non-canonical NF-κB pathways demonstrates significant anti-tumor activities in multiple myeloma

Claire Fabre[1], **Naoya Mimura**[1], **Kathryn Bobb**[2], **Sun-Young Kong**[1,3], **Güllü Gorgun**[1], **Diana Cirstea**[1], **Yiguo Hu**[1], **Jiro Minami**[1], **Hiroto Ohguchi**[1], **Jie Zhang**[4], **Jeffrey Meshulam**[2], **Ruben D. Carrasco**[5], **Yu-Tzu Tai**[1], **Paul G. Richardson**[1], **Teru Hideshima**[1], and **Kenneth C. Anderson**[1]

[1]Jerome Lipper Multiple Myeloma Center, Department of Medical Oncology, Dana-Farber Cancer Institute, Harvard Medical School, Boston, MA, United States

[2]Profectus BioSciences Inc., Baltimore, MD, United States

[3]Research Institute and Hospital, National Cancer Center, Korea

[4]rel~MD, Inc., Baltimore, MD, United States

[5]Department of Medical Oncology, Dana-Farber Cancer Institute, Harvard Medical School, Boston, MA, United States

Abstract

Purpose—NF-κB transcription factor plays a key role in the pathogenesis of multiple myeloma (MM) in the context of the bone marrow (BM) microenvironment. Both canonical and non-canonical pathways contribute to total NF-κB activity. Recent studies have demonstrated a critical role for the non-canonical pathway: selective inhibitors of the canonical pathway present a limited activity, mutations of the non-canonical pathway are frequent, and bortezomib-induced cytotoxicity cannot be fully attributed to inhibition of canonical NF-κB activity.

Experimental design—MM cell lines, primary patient cells, and the human MM xenograft murine model were used to examine the biologic impact of dual inhibition of both canonical and non-canonical NF-κB pathways.

Results—We show that PBS-1086 induces potent cytotoxicity in MM cells, but not in peripheral blood mononuclear cells. PBS-1086 overcomes the proliferative and anti-apoptotic effects of the BM milieu, associated with inhibition of NF-κB activity. Moreover, PBS-1086 strongly enhances the cytotoxicity of bortezomib in bortezomib-resistant MM cell lines and patient MM cells. PBS-1086 also inhibits osteoclastogenesis through an inhibition of RANKL-induced NF-κB

Correspondence: Kenneth C. Anderson, M.D., Jerome Lipper Multiple Myeloma Center, Department of Medical Oncology, Dana-Farber Cancer Institute, 450 Brookline Avenue, 02215 Boston (MA), United States, kenneth_anderson@dfci.harvard.edu.

Conflict of interest disclosure: K.B., J.Z., and J.M. are employees of Profectus and rel~MD, which produce PBS1086.

Authorship contributions: C.F. and T.H. designed research, performed experiments, analyzed data, and wrote the manuscript; N.M., K.B., and S-Y.K. performed experiments and analyzed data; G.G., D.C., Y.H., J.M., H.O., and R.D.C. helped in the interpretation of data; J.Z. and J.M. provided the compound, designed dosing regimen, and analyzed data; Y-T.T. and P.G.R. provided clinical samples; and K.C.A. designed research, analyzed data, and wrote the manuscript.

activation. Finally, in a xenograft model of human MM in the BM milieu, PBS-1086 shows significant *in vivo* anti-MM activity and prolongs host survival, associated with apoptosis and inhibition of both NF-κB pathways in tumor cells.

Conclusions—Our data demonstrate that PBS-1086 is a promising dual inhibitor of the canonical and non-canonical NF-κB pathways. Our preclinical study therefore provides the framework for clinical evaluation of PBS-1086 in combination with bortezomib for the treatment of MM and related bone lesions.

Keywords

multiple myeloma; NF-κB; Rel inhibitors; canonical and non-canonical pathways

INTRODUCTION

Multiple myeloma (MM) is a clonal proliferation of malignant plasma cells that accounts for 1% of all cancers and more than 10% of all hematological malignancies. Pure osteolytic bone lesions are pathognomonic of MM and affect more than 80% of patients (1). Proteasome inhibitors (bortezomib) have dramatically changed MM prognosis by overcoming drug resistance to conventional treatments (2). However, resistance to bortezomib ultimately occurs, highlighting the urgent need for new therapeutic approaches (3).

NF-κB transcription factors play a key role in the pathogenesis of cancers, including MM, by regulating genes involved in proliferation, survival, and drug resistance (4, 5). Constitutive NF-κB activity is present in human MM cell lines and patient MM cells (6, 7); moreover, adhesion of MM cells to bone marrow stromal cells (BMSCs) induces NF-κB-dependent cytokine (IL-6, TNF-α, IL1-β, SDF-1α, BAFF) transcription and secretion by BMSCs, which in turn further activates NF-κB and thereby promotes MM cell growth and survival (6, 8–10). NF-κB also modulates expression of anti-apoptotic proteins and adhesion molecules such as ICAM-1 (CD54) and VCAM-1 (CD106) on both MM and BMSCs, further enhancing adhesion of MM cells to BMSCs (11). Finally, NF-κB pathway plays an important role in bone osteolytic lesions, mostly *via* RANK (receptor activator of NF-κB)/RANK ligand (RANKL)-mediated activation of osteoclasts (OC) (12, 13). These studies validate NF-κB pathway as a promising therapeutic target in MM.

In MM, NF-κB is constitutively present in the cytoplasm in a latent inactive form through its interaction with inhibitory IκB proteins. After stimulation *via* the canonical pathway, IκB is phosphorylated by IKK complex at 2 specific N-terminal serine residues (Ser32 and Ser36), leading to their ubiquitination and degradation by the 26S proteasome. Rel/NF-κB complex is then released and translocates into the nucleus, where it binds to DNA to activate transcription of various target genes. Several studies also demonstrate a critical role for the non-canonical NF-κB pathway in MM pathogenesis (14). Using an 11-gene expression signature for NF-κB activation, recent studies correlated constitutive NF-κB activity with mutations in regulators of NF-κB (CD40, NIK, TRAF2, TRAF3) (15–17). Overall mutations involving both canonical and non-canonical NF-κB pathways are present in at least 17% of MM patient samples and 40% of MM cell lines, enabling MM cells to become less

dependent on extrinsic signals from the BM microenvironment. Moreover, mutations of the non-canonical pathway in 20% of MM, are associated with resistance to steroids *versus* sensitivity to proteasome inhibitors.

To date, the canonical NF-κB pathway can be blocked by small-molecule inhibitors of IKKβ (e.g. PS-1145, MLN120B), which inhibit MM cell growth *in vitro*. However, *in vivo* anti-MM activity of IKKβ inhibitors is limited due to the compensatory activation of the non-canonical pathway (7, 18). Moreover, bortezomib inhibits inducible NF-κB activity in MM cells, but unexpectedly enhances constitutive NF-κB activity *via* activation of the canonical pathway. Therefore, bortezomib-induced cytotoxicity cannot be fully attributed to inhibition of canonical NF-κB activity in MM cells (19, 20). Since inhibition of both canonical and non-canonical pathways is required to efficiently block total NF-κB activity, we here characterize the anti-tumor activity of PBS-1086, an inhibitor of both canonical and non-canonical NF-κB pathways (21), in MM.

MATERIALS AND METHODS

Reagents

PBS-1086 was provided by Profectus BioSciences Inc. (Baltimore, MD). Bortezomib was obtained from Selleck Chemicals (Houston, TX). Doxorubicin and z-Val-Ala-Asp-fluoromethylketone (z-VAD-fmk) were obtained from Sigma Aldrich (St. Louis, MO). TNF-α, insulin-like growth factor I (IGF-I), and recombinant IL-6 were purchased from R&D Systems (Minneapolis, MN).

Human MM cell lines

Dexamethasone (Dex)-sensitive (MM.1S) and Dex-resistant (MM.1R) cell lines were kindly provided by Dr. Steven Rosen (Northwestern University, Chicago, IL); RPMI 8226 and U266 were purchased from the ATCC; Doxorubicin-resistant RPMI-Dox40 (Dox40) and melphalan-resistant RPMI-LR5 (LR5) cell lines were provided by Dr. William Dalton (Moffitt Cancer Center, Tampa, FL); KMS18 by the DSMZ; IL-6 dependent INA6 by Dr. Renate Burger (University of Kiehl, Germany); and bortezomib-resistant IL-6 dependent cell line ANBL6-VR5 and its parental counterpart ANBL6-wt by Dr. Robert Orlowski (MD Anderson Cancer Center, Houston, TX). All MM cell lines were cultured in RPMI-1640 containing 10% fetal bovine serum (FBS, Sigma Chemical Co.) (20% FBS for ANBL6), 2 μM L-glutamine, 100 U/mL penicillin, and 100 μg/mL streptomycin (GIBCO). INA6 and ANBL6 cell lines were cultured with IL-6 at 2.5 and 5 ng/ml, respectively.

Tumor cells and BMSCs from MM patients

Blood samples from healthy volunteers were processed by Ficoll Hypaque (GE Healthcare) gradient to obtain peripheral blood mononuclear cells (PBMC) and stimulated by phytohemagglutinin. Tumor cells and BMSCs from MM patients were obtained from BM aspirates after informed consent as per the Declaration of Helsinki and approval by the Institutional Review Board of the Dana-Farber Cancer Institute. Mononuclear cells were separated using Ficoll Hypaque density sedimentation, and plasma cells were purified (> 95% CD138+) by positive selection with anti-CD138 magnetic activation cell separation

microbeads (Miltenyi Biotech). BMSCs were generated by culturing BM mononuclear cells for 4–6 weeks in DMEM containing 15% FBS, 2 μM L-glutamine, 100 U/ml penicillin, and 100 μg/ml streptomycin.

Osteoclasts cultivation and differentiation assay

PBMC were isolated as described above and cultured in α-MEM containing 10% FCS, 100 U/ml penicillin, 100 μg/ml streptomycin, 25 ng/ml macrophage colony-stimulating factor (M-CSF) (R&D Systems), and 25 ng/ml RANKL (PeproTech). After 24 hours, the adherent population was reseeded in 96-well plates. After a culture period of 14–21 days, cells were stained for TRAP activity, using a Leukocyte Acid Phosphatase Kit (Sigma Aldrich). Histologic micrographs were taken using a Leica DM200 microscope (aperture HC PLANs 10x/22, objective lenses: N PLAN 10x), and a SPOT/insight QE model camera with SPOT advanced acquisition software (Diagnostic Instruments, Sterling Heights). Mature OC were identified as large multi-nucleated (> 2 nuclei) TRAP-positive cells and quantified by light microscopy.

Growth inhibition assay

The growth inhibitory effect of PBS-1086 on MM or OC cell growth was assessed by measuring 3-(4,5-dimethylthiazol-2-yl)-2,5-diphenyl tetrasodium bromide (MTT, Sigma Aldrich) dye absorbance. Cells were pulsed with MTT for the last 4 hours of culture, followed by isopropanol containing 0.04 N HCl. Absorbance was measured at 570/630 nm using a spectrophotometer.

Detection of cytokines

Bone serological marker TRAP5b (tartrate-resistant acid phosphatase 5b) (22) was measured by ELISA (TRAP5b: Quidel) in culture supernatants from OC, with or without PBS-1086.

Detection of apoptosis by Annexin V/Propidium iodide (PI)

Detection of apoptosis was performed with the Annexin V-FITC/PI detection kit (Immunotech/Beckman Coulter), as previously described. Apoptotic cells were enumerated using the FACSCalibur flow cytometer (Becton Dickinson). Annexin V-FITC single-positive cells were considered to be early apoptotic, PI single-positive cells necrotic, and Annexin V-FITC double-positive cells late apoptotic.

DNA synthesis

DNA synthesis was measured by [^{3}H]-thymidine ([^{3}H]-TdR, Perkin Elmer) uptake to evaluate growth of MM cells adherent to BMSCs in BMSC-coated 96-well plates. Cells were pulsed with [^{3}H]-TdR (0.5 μCi/well) during the last 8 hours of culture, harvested onto glass filters with an automatic cell harvester (Cambridge Technology), and counted using the Betaplate scintillation counter.

Cytoplasmic and nuclear fractionation

Cytoplasmic and nuclear fractionation was performed using the nuclear extract kit (Panomics), according to the manufacturer's instructions. For BMSC co-culture, MM cells

were incubated in BMSCs-coated flasks for 12 hours, harvested by pipetting, and subjected to nuclear protein extraction.

NF-κB DNA-binding ELISA

DNA-binding activity of NF-κB was quantified by ELISA using the Trans-AM NF-κB Family Transcription Factor Assay Kit (Active Motif), according to the manufacturer's instructions. Briefly, nuclear extracts were transferred to a 96-well plate coated with NF-κB consensus oligonucleotides. NF-κB proteins bound to the target sequence were detected with primary antibodies specific for each Rel member and an HRP-conjugated secondary antibody. Absorbance was measured at 595 nm as a relative measure of protein bound NF-κB. Specificity was confirmed by the use of wild-type and mutant NF-κB oligonucleotide competitors.

Immunoblotting

MM cells or mature OC were treated with or without therapeutic agents. Cells were then harvested, washed, and lysed, as in prior studies. Whole cell lysates were subjected to SDS-PAGE, transferred to membranes, and immunoblotted with antibodies against: caspase 3, caspase 7, caspase 8, caspase 9, PARP, IκBα, phospho-IκBα (Ser32/36), ERK, c-Jun-NH2-terminal kinase (JNK), p38/MAPK, and GAPDH (Cell Signaling Technology); as well as p50, p52, p65, RelB, c-Rel, nucleolin and α-tubulin (Santa Cruz Biotechnology). Densitometric analyses of scanned immunoblotting images were performed with the NIH Image J Software.

Osteoclast activity assay

The bone resorption activity of OC was measured using the Bone Resorption Assay Plate (Cosmo Bio). OC precursors obtained from patient BM samples were seeded in the calcium phosphate-coated 24-well plates in α-MEM containing 10% FCS, 25 ng/ml M-CSF, and 50 ng/ml RANKL; PBS-1086 was added at the indicated doses. After a culture period of 14–21 days, the 24-well plate was processed as directed by manufacturer. Pit resorption areas corresponded to dark areas where calcium phosphate was resorbed as opposed to bright areas where calcium phosphate layer remained intact. Mean pit resorption areas were determined by light microscopy and quantified by using NIH ImageJ program. Histologic micrographs were taken using a Leica DM200 microscope (aperture HC PLANs 10x/22, objective lenses: N PLAN 10x) and a SPOT/insight QE model camera with SPOT advanced acquisition software (Diagnostic Instruments, Sterling Heights). The average pit resorption area is indicated as percentage of control (osteoclasts stimulated with M-CSF and RANKL).

Murine xenograft model of human MM

CB17 SCID mice (6–8 week-old male) were purchased from Charles River Laboratories, Inc. All animal studies were conducted according to protocols approved by and conform to the relevant regulatory standards of the Institutional Animal Care and Use Committee of the Dana-Farber Cancer Institute. Mice were injected subcutaneously with 5×10^6 MM.1S cells in 100 μl FCS-free RPMI-1640 medium. When tumor was measurable, mice were assigned into 6 treatment groups: PBS-1086 (at 7.5 mg/kg), bortezomib, PBS-1086 (at 2.5 or 7.5

mg/kg) with bortezomib, vehicle (20% DMSO/80% Cremophor), and control (100% saline). PBS-1086 was given IP once daily, 5 days/week for 4 weeks. Control and vehicle were administered IP with the same schedule. Bortezomib was given IV at 0.5 mg/kg twice a week for 4 weeks. Each group consisted of at least 8 tumor-bearing mice. Tumor volume was calculated from caliper measurements three times per week, using the following formula: $V = 0.5\ a \times b^2$ where a and b are the long and short diameters of the tumor, respectively. Mice were euthanized when tumor volume reached 2 cm^3. Survival was evaluated from the first day of treatment until death.

In situ detection of apoptosis and immunohistochemistry

Sections from harvested tumors were subjected to immunohistochemical (IHC) staining for terminal deoxynucleotidyltransferase-mediated dUTP nick end labeling (TUNEL) for detection of apoptosis. Ki67 was also assessed by IHC staining to quantify proliferation.

Statistical analysis

Statistical significance was determined by sample t test and test for equal variance. The minimal level of significance was $p<0.05$. Overall survival was analyzed by Kaplan-Meier method. The Kaplan-Meier curves were constructed for each group using GraphPad Prism software, and the log-rank (Mantel-Cox) test was used to compare survival curves among groups. The combined effect of PBS-1086 with bortezomib was analyzed by isobologram analysis using the CompuSyn software program (ComboSyn, Inc).

RESULTS

PBS-1086 inhibits both canonical and non-canonical NF-κB pathways

We first evaluated the effect of PBS-1086 (chemical structure in Figure 1A) on NF-κB activity in MM cells. PBS-1086 inhibited the binding of all Rel proteins to DNA. At 0.1 μM PBS-1086, p65 and p50 were inhibited by 62% and 56%, compared to 28% and 22% inhibition of p52 and RelB (Figure 1B). To evaluate the kinetics of NF-κB inhibition, MM.1S cells were treated with PBS-1086 for 0.5 to 12 hours. PBS-1086 inhibited NF-κB binding to DNA even after a short exposure, with potent inhibition of p65, p50 (90–95%), p52 (63%), and RelB (79%) (Figure 1C). Dose- and time-dependent NF-κB inhibition after PBS-1086 treatment was also confirmed in MM.1S cells (Figure 1D). Inhibition of NF-κB activity by PBS-1086 in additional MM cell lines is demonstrated in Supplemental Figure S1A (KMS18) and S1B (INA6). We examined the expression of p65, p50, and p52 in cytoplasmic and nuclear extracts from MM.1S cells treated with PBS-1086 by Western blotting (Figure 1E). A time-dependent decrease in expression of NF-κB proteins was observed in nuclear extracts, whereas cytoplasmic protein remained stable (Figure 1F), confirming that PBS-1086 acts through an inhibition of NF-κB translocation into the nucleus. Furthermore, PBS-1086 did not inhibit the phosphorylation and degradation of IκBα in MM cells (Supplemental Figure S2). Altogether, these data confirm that PBS-1086 blocks both canonical and non-canonical NF-κB pathways in MM cell lines in a dose- and time-dependent manner.

PBS-1086 induces cytotoxicity and apoptosis in MM cells

We next investigated the growth inhibitory effect of PBS-1086 *in vitro*. Treatment of MM cells with PBS-1086 for 48 hours induced a dose-dependent decrease in cell viability, with IC50 values of PBS-1086 ranging from 0.31 to 5 μM (Figure 2A). Cells vary in their baseline NF-κB activity (19) and included sensitive cells (MM.1S, INA6, KMS18 with IC50 0.31–0.62 μM), intermediate sensitive cells (MM.1R, Dox40, RPMI 8226 with IC50 1.25–2.5 μM), and resistant cells (LR5, U266 with IC50 2.5–5 μM). However, growth inhibitory effect of PBS-1086 was observed in MM cell lines irrespective of their sensitivity or resistance to conventional treatments or their genetic background. A similar growth inhibitory effect was observed in four patient MM cells treated for 48 hours with PBS-1086 (Figure 2B). Normal PBMCs from four healthy volunteers and stimulated by phytohemagglutinin were treated for 48 hours with PBS-1086 and similarly analyzed for cytotoxicity. PBS-1086 showed only modest cytotoxicity on normal PBMCs, with a maximum viability loss of 10% at 1.25 μM (Figure 2C) and IC50 0.62–1.25 μM, indicating a higher sensitivity of tumor cells than PBMCs to PBS-1086. These results suggest that PBS-1086 potently inhibits the growth of MM cell lines in a dose-dependent manner, with a favorable therapeutic window. To determine molecular mechanisms whereby PBS-1086 induces cytotoxicity in MM cells, MM.1S cells treated with PBS-1086 were analyzed for apoptosis using Annexin V-PI staining. PBS-1086 significantly increased Annexin V(+)/PI(−) in MM.1S cells in a time- and dose-dependent manner (Figure 2D). Moreover, PBS-1086 triggered cleavage of caspase-8, caspase 3/7 and PARP, indicating that the intrinsic apoptotic pathway was predominantly activated by PBS-1086 (Figure 2E). Conversely, pan-caspase inhibitor z-VAD-fmk markedly abrogated PBS-1086-induced apoptosis, confirming that PBS-1086-induced cytotoxicity is mediated, at least in part, *via* caspase-dependent apoptosis (Figure 2F). Taken together, these results show that PBS-1086 induced apoptosis in MM cells.

PBS-1086 overcomes the proliferative and anti-apoptotic effects of BMSCs associated with inhibition of NF-κB

Since IL-6 and IGF-I are major growth and/or survival factors in the BM milieu (8, 23–28), we examined their effect on PBS-1086-induced apoptosis. Even with exogenous IL-6 or IGF-I, PBS-1086 induced cytotoxicity (Figures 3A and 3B). In a dose-dependent manner, PBS-1086 also inhibited growth of MM.1S cells cocultured with BMSCs (Figure 3C). We next investigated whether PBS-1086 could inhibit NF-κB inducible activity in the BM microenvironment. Coculture of MM.1S cells with BMSCs activated NF-κB, predominantly *via* the canonical pathway, which was significantly inhibited by PBS-1086 (Figure 3D). We also investigated the effect of PBS-1086 on BMSCs. Importantly, PBS-1086 inhibited both canonical and non-canonical NF-κB pathways in BMSCs. Altogether, these results demonstrate that PBS-1086 targets not only MM cells, but also the BM microenvironment to overcome the proliferative and anti-apoptotic effects of BMSCs.

PBS-1086 enhances cytotoxicity of bortezomib in bortezomib-resistant MM cells

We next evaluated the combination of PBS-1086 with bortezomib in bortezomib-resistant MM cell lines. Combining PBS-1086 with bortezomib triggered synergistic cytotoxicity

against Dox40 (Figure 4A and Supplemental Table S3) and ANBL6-VR5 (Figure 4B and Supplemental Table S3) cells. For example, PBS-1086 (0.31 μM) and bortezomib (20 nM) triggered 8% and 35% cytotoxicity, whereas PBS-1086 with bortezomib at the same concentrations induced 52% cytotoxicity (Figure 4B). In bortezomib-resistant patient MM cells, combining PBS-1086 with bortezomib markedly decreased MM cell viability (Figure 4C), suggesting that PBS-1086 overcomes bortezomib resistance (Supplemental Figure S4). We further investigated the effect of PBS-1086/bortezomib combination on NF-κB activity in bortezomib-resistant ANBL6-VR5 cells. The binding activity of Rel proteins was similar in bortezomib-treated and control cells (Figure 4D). Moreover, bortezomib-induced activation of canonical NF-κB pathway was inhibited by PBS-1086 (Figures 4D and 4E). No overexpression in hsp27, which has been associated with bortezomib resistance (29) (data not shown), nor change in p38, an upstream effector of hsp27 (30, 31), was observed in ANBL6-VR5 cells after PBS-1086 treatment (Supplemental Figure S4).

PBS-1086 inhibits osteoclast activity associated with inhibition of NF-κB

We also investigated the effect of PBS-1086 on OC. PBS-1086 did not induce cytotoxicity in OC, as evidenced by both MTT and 3H-thymidine uptake (Figures 5A and 5B). To examine the effect of PBS-1086 on OC differentiation, mature OC were treated with PBS-1086, followed by TRAP assay. PBS-1086 inhibited OC differentiation in a dose-dependent manner (Figure 5C). To evaluate the effect of PBS-1086 on OC activity, we quantified TRAP5b in the culture supernatants of mature OC treated with PBS-1086: 15% and 25% reduction in TRAP5b activity was observed at 1.25 μM and 5 μM, respectively (Figure 5D). Functional osteoclast activity resorbing bone substrate was also assessed using calcium-phosphate coated plates. PBS-1086 inhibited the bone resorption activity of mature OC in a dose-dependent manner, with 75% and 100% decrease in pit area at 1.25 and 5 μM PBS-1086, respectively (Figure 5E). Finally, we investigated whether the inhibitory effect of PBS-1086 on osteoclastogenesis was due to inhibition of NF-κB. Mature OC exhibited high baseline p50 expression in the nucleus (Figure 5F), suggesting that NF-κB activity in mature OC is maintained *via* the canonical pathway. Importantly, PBS-1086 inhibited both p50 and p52 NF-κB in a dose-dependent manner. No change of p38MAPK, JNK, and ERK, other pathways mediating osteoclastogenesis (32, 33), was observed (Supplemental Figure S5). Taken together, our results indicate that PBS-1086 inhibits RANKL-induced osteoclastogenesis, associated with inhibition of NF-κB.

PBS-1086 inhibits tumor growth in a murine xenograft model of human MM

Finally, we investigated the effect of PBS-1086 in combination with bortezomib on MM.1S cell growth in a murine xenograft model of human MM cells. Mice were injected subcutaneously with MM.1S cells that exhibit both canonical and non-canonical NF-κB pathways. In combination with bortezomib, PBS-1086 significantly inhibited tumor growth *versus* control (2.5 mg/kg, p=0.00039 and 7.5 mg/kg, p=0.00084) (Figure 6A). Tumor growth was also significantly reduced in PBS-1086 with bortezomib *versus* bortezomib alone (2.5 mg/kg, p=0.00325 and 7.5 mg/kg, p=0.0057) treated cohorts. Importantly, treatment with PBS-1086 and bortezomib prolonged overall survival *versus* control (2.5 mg/kg, p=0.0133 and 7.5 mg/kg, p=0.0121). Overall survival was also significantly increased in PBS-1086 and bortezomib groups *versus* bortezomib alone (2.5 mg/kg,

p=0.0151 and 7.5 mg/kg, *p*=0.0307) (Figure 6B). With a median follow-up of 140 days (range 28–170), 50% mice receiving PBS-1086 7.5 mg/kg and bortezomib were alive with no detectable tumor. Overall, treatment with PBS-1086, alone or in combination, was well tolerated, with no significant body weight changes compared to control group (Figure 6C). IHC staining for NF-κB on excised tumor showed time-dependent inhibition of both canonical and non-canonical NF-κB pathways, with significantly decreased expression of p65, p50, and p52 in the nucleus in tumor cells harvested from PBS-1086 treated mice (data not shown). PBS-1086 also induced time-dependent apoptosis (TUNEL staining) and decrease in proliferation (Ki67 staining) *in vivo* (data not shown). Altogether, our *in vivo* study demonstrates that inhibition of NF-κB by PBS-1086 is associated with significant *in vivo* anti-MM activity and improved overall survival.

DISCUSSION

NF-κB transcription factors play a critical role in the pathogenesis of MM, since constitutive NF-κB activation promotes cell growth, survival, and drug resistance (6). NF-κB is involved in the intimate crosstalk between MM cells, the BM microenvironment, and the bone matrix (34). Consequently, targeting direct NF-κB is a promising treatment strategy in MM. The importance of NF-κB non-canonical pathway in MM has been confirmed both by the frequency of mutations affecting this pathway (15, 16, 18) and the limited activity of IKKβ inhibitors of the canonical pathway (18). Therefore, inhibition of both canonical and non-canonical NF-κB pathways is necessary to achieve complete blockade of NF-κB activity. In the present study, we investigated the effect of PBS-1086, a dual NF-κB inhibitor. PBS-1086 binds to Rel proteins to form covalent bonds with cysteine 38 in RelA (p65), cysteine 144 in RelB or cysteine 67 in c-Rel to inhibit binding of Rel to the κB sites in DNA (35).

We first confirmed that PBS-1086 strongly inhibits both canonical and non-canonical NF-κB pathways in MM cells. MTT evaluation in MM cell lines and patient CD138+ MM cells shows a selective effect on MM, with a favorable therapeutic index. PBS-1086 induces apoptosis in MM cells through activation of the intrinsic apoptotic pathway. Partial reversibility of cell killing in the presence of a pancaspase inhibitor z-VAD-fmk suggests that PBS-1086 might also trigger signaling pathways other than caspases. PBS-1086 induces synergistic cytotoxicity in combination with bortezomib in bortezomib-resistant MM cells and in patient MM cells refractory to bortezomib. Overexpression of hsp27 confers bortezomib resistance (29); however, this mechanism was not observed in ANBL6-VR5 cell line. We did not determine whether PBS-1086 might interfere with additional mechanisms contributing to bortezomib resistance, such as mutations of proteasome subunits or increased activity of the aggresome pathway (36, 37). In combination with bortezomib, PBS-1086 induced potent anti-MM activity *in vivo* in a murine xenograft model of human MM, with significant tumor growth reduction. Importantly, significantly prolonged overall survival was observed in PBS-1086/bortezomib combination treatment groups. IHC analysis of harvested tumors demonstrated that PBS-1086 anti-MM activity *in vivo* was associated with dual inhibition of NF-κB pathway in tumor cells. Altogether, our results suggest a broad clinical applicability of PBS-1086 to overcome bortezomib resistance not only in MM, but also in other hematologic malignancies and solid tumors as well (38).

Several studies have emphasized the role of the BM microenvironment in promoting drug resistance, demonstrating the need for anti-MM agents to target not only MM cells, but also BMSCs(39). In the BM milieu, TNF-α is secreted by MM cells and induces NF-κB-dependent expression of adhesion molecules on both MM cells and BMSCs, further increasing cell adhesion (11). Enhanced binding in turn confers resistance to apoptosis and triggers NF-κB-dependent secretion of cytokines (11). Our data demonstrate that PBS-1086 inhibits both constitutive and inducible NF-κB activity in MM cells and in BMSCs. Our laboratory has previously shown that bortezomib inhibits TNF-α-induced NF-κB activation (18). However, some MM cells have constitutive activation of NF-κB through proteasome inhibitor-resistant pathways, leading to bortezomib resistance due to both constitutive and inducible NF-κB activities (40). Our data show, unlike bortezomib, that PBS-1086 might be efficacious even when proteasome inhibitor-resistant pathways are activated. Moreover, during MM progression, mutations of the NF-κB pathway lead to decreased dependence on extrinsic signals from the BM microenvironment (41). Importantly, our data further suggest that PBS-1086 might prevent MM progression by inhibition of TNF-α-induced NF-κB activation. Finally, we did not show any significant inhibitory effect of PBS-1086 on IL-6 secretion within the BM milieu, even though NF-κB is involved in the transcriptional regulation of IL-6 expression in MM cells (8). Recently, some authors have reported constitutive expression of IL-6 regulated by several transcription factors besides NF-κB, with no requirement for NF-κB binding activity to DNA (42, 43). The effect of PBS-1086, at least on paracrine IL-6 secretion, requires further investigation.

The role of NF-κB signaling in bone pathogenesis is primarily *via* RANKL/RANK-induced activation of NF-κB pathway (12). Mice deficient in both p50 and p52 subunits, which are deficient in total NF-κB activity, develop severe osteopetrosis due to the absence of OC formation (44–46). In contrast, deletion of either p50 or p52 causes no detectable bone phenotype, with intact OC formation (47). Dominant negative mutant IKKβ leads to inhibition of NF-κB canonical pathway and results in decreased OC differentiation (48). Here we show that PBS-1086 inhibits both the differentiation and function of OC by inhibition of both canonical and non-canonical NF-κB pathways. The inhibitory effect on bone resorption was more potent than on OC differentiation, consistent with dual inhibition of NF-κB and more potent inhibition of the canonical pathway. Since RANKL/RANK binding can also activate other signaling pathways including p38/MAPK (32), JNK, and ERK(49), we confirmed that the inhibitory effect of PBS-1086 on osteoclastogenesis was specific to NF-κB inhibition. Bortezomib inhibits osteoclastogenesis through different pathways dependent on OC differentiation status, with inhibition of p38/MAPK at early stages and inhibition of other pathways including NF-κB at later stages (49, 50). Therefore, we cannot exclude that PBS-1086 might also indirectly affect NF-κB independent pathways at earlier stages of osteoclastogenesis *in vivo*. Importantly, besides its direct cytotoxicity on MM cells, PBS-1086 exerts an indirect inhibitory effect on the BM milieu and bone matrix, thereby disrupting tumor-BM milieu interactions which contribute to MM progression.

In conclusion, our study demonstrates that PBS-1086 is a promising dual inhibitor of the canonical and non-canonical NF-κB pathways. Besides its potent and selective cytotoxicity on MM cells, PBS-1086 also targets the BM microenvironment and overcomes the

proliferative and anti-apoptotic effects of BMSCs, associated with an inhibition of TNF-α-inducible NF-κB activation. In addition, we show that PBS-1086 is synergistic with bortezomib against bortezomib-resistant MM cells and patient MM cells refractory to bortezomib. Finally, PBS-1086 inhibits RANKL-induced osteoclastogenesis, associated with an inhibition of NF-κB pathway. Our data therefore provide the framework for clinical evaluation of PBS-1086 in combination with bortezomib for the treatment of MM and related bone lesions.

Supplementary Material

Refer to Web version on PubMed Central for supplementary material.

Acknowledgements

We thank Dharminder Chauhan, Catriona Hayes, Constantine Mitsiades, and Loredana Santo for helpful suggestions.

REFERENCES

1. Roodman GD. Pathogenesis of myeloma bone disease. Leukemia. 2009; 23(3):435–41. [PubMed: 19039321]
2. Richardson PG, Barlogie B, Berenson J, Singhal S, Jagannath S, Irwin D, et al. A phase 2 study of bortezomib in relapsed, refractory myeloma. N Engl J Med. 2003; 348(26):2609–17. [PubMed: 12826635]
3. Laubach J, Richardson P, Anderson K. Multiple myeloma. Annu Rev Med. 2011; 62:249–64. [PubMed: 21090965]
4. Hideshima T, Anderson KC. Molecular mechanisms of novel therapeutic approaches for multiple myeloma. Nat Rev Cancer. 2002; 2(12):927–37. [PubMed: 12459731]
5. Gilmore TD. Multiple myeloma: lusting for NF-kappaB. Cancer Cell. 2007; 12(2):95–7. [PubMed: 17692798]
6. Hideshima T, Chauhan D, Richardson P, Mitsiades C, Mitsiades N, Hayashi T, et al. NF-kappa B as a therapeutic target in multiple myeloma. J Biol Chem. 2002; 277(19):16639–47. [PubMed: 11872748]
7. Hideshima T, Neri P, Tassone P, Yasui H, Ishitsuka K, Raje N, et al. MLN120B, a novel IkappaB kinase beta inhibitor, blocks multiple myeloma cell growth in vitro and in vivo. Clin Cancer Res. 2006; 12(19):5887–94. [PubMed: 17020997]
8. Chauhan D, Uchiyama H, AkBarali Y, Urashima M, Yamamoto K, Libermann TA, et al. Multiple myeloma cell adhesion-induced interleukin-6 expression in bone marrow stromal cells involves activation of NF-kappa B. Blood. 1996; 87(3):1104–12. [PubMed: 8562936]
9. Jourdan M, Moreaux J, Vos JD, Hose D, Mahtouk K, Abouladze M, et al. Targeting NF-kappaB pathway with an IKK2 inhibitor induces inhibition of multiple myeloma cell growth. Br J Haematol. 2007; 138(2):160–8. [PubMed: 17542984]
10. Landowski TH, Olashaw NE, Agrawal D, Dalton WS. Cell adhesion-mediated drug resistance (CAM-DR) is associated with activation of NF-kappa B (RelB/p50) in myeloma cells. Oncogene. 2003; 22(16):2417–21. [PubMed: 12717418]
11. Hideshima T, Chauhan D, Schlossman R, Richardson P, Anderson KC. The role of tumor necrosis factor alpha in the pathophysiology of human multiple myeloma: therapeutic applications. Oncogene. 2001; 20(33):4519–27. [PubMed: 11494147]
12. Boyle WJ, Simonet WS, Lacey DL. Osteoclast differentiation and activation. Nature. 2003; 423(6937):337–42. [PubMed: 12748652]

13. Novack DV, Yin L, Hagen-Stapleton A, Schreiber RD, Goeddel DV, Ross FP, et al. The IkappaB function of NF-kappaB2 p100 controls stimulated osteoclastogenesis. J Exp Med. 2003; 198(5): 771–81. [PubMed: 12939342]

14. Sun SC. Non-canonical NF-kappaB signaling pathway. Cell Res. 2011; 21(1):71–85. [PubMed: 21173796]

15. Annunziata CM, Davis RE, Demchenko Y, Bellamy W, Gabrea A, Zhan F, et al. Frequent engagement of the classical and alternative NF-kappaB pathways by diverse genetic abnormalities in multiple myeloma. Cancer Cell. 2007; 12(2):115–30. [PubMed: 17692804]

16. Keats JJ, Fonseca R, Chesi M, Schop R, Baker A, Chng WJ, et al. Promiscuous mutations activate the noncanonical NF-kappaB pathway in multiple myeloma. Cancer Cell. 2007; 12(2):131–44. [PubMed: 17692805]

17. Demchenko YN, Glebov OK, Zingone A, Keats JJ, Bergsagel PL, Kuehl WM. Classical and/or alternative NF-kappaB pathway activation in multiple myeloma. Blood. 2010; 115(17):3541–52. [PubMed: 20053756]

18. Hideshima T, Chauhan D, Kiziltepe T, Ikeda H, Okawa Y, Podar K, et al. Biologic sequelae of I{kappa}B kinase (IKK) inhibition in multiple myeloma: therapeutic implications. Blood. 2009; 113(21):5228–36. [PubMed: 19270264]

19. Hideshima T, Ikeda H, Chauhan D, Okawa Y, Raje N, Podar K, et al. Bortezomib induces canonical nuclear factor-kappaB activation in multiple myeloma cells. Blood. 2009; 114(5):1046–52. [PubMed: 19436050]

20. Li C, Chen S, Yue P, Deng X, Lonial S, Khuri FR, et al. Proteasome inhibitor PS-341 (bortezomib) induces calpain-dependent IkappaB(alpha) degradation. J Biol Chem. 2010; 285(21):16096–104. [PubMed: 20335171]

21. Oh U, McCormick MJ, Datta D, Turner RV, Bobb K, Monie DD, et al. Inhibition of immune activation by a novel nuclear factor-kappa B inhibitor in HTLV-I-associated neurologic disease. Blood. 2011; 117(12):3363–9. [PubMed: 21212284]

22. Halleen JM, Alatalo SL, Suominen H, Cheng S, Janckila AJ, Vaananen HK. Tartrate-resistant acid phosphatase 5b: a novel serum marker of bone resorption. J Bone Miner Res. 2000; 15(7):1337–45. [PubMed: 10893682]

23. Hideshima T, Nakamura N, Chauhan D, Anderson KC. Biologic sequelae of interleukin-6 induced PI3-K/Akt signaling in multiple myeloma. Oncogene. 2001; 20(42):5991–6000. [PubMed: 11593406]

24. Catlett-Falcone R, Landowski TH, Oshiro MM, Turkson J, Levitzki A, Savino R, et al. Constitutive activation of Stat3 signaling confers resistance to apoptosis in human U266 myeloma cells. Immunity. 1999; 10(1):105–15. [PubMed: 10023775]

25. Ogata A, Chauhan D, Teoh G, Treon SP, Urashima M, Schlossman RL, et al. IL-6 triggers cell growth via the Ras-dependent mitogen-activated protein kinase cascade. J Immunol. 1997; 159(5): 2212–21. [PubMed: 9278309]

26. Mitsiades CS, Mitsiades N, Poulaki V, Schlossman R, Akiyama M, Chauhan D, et al. Activation of NF-kappaB and upregulation of intracellular anti-apoptotic proteins via the IGF-1/Akt signaling in human multiple myeloma cells: therapeutic implications. Oncogene. 2002; 21(37):5673–83. [PubMed: 12173037]

27. Hideshima T, Mitsiades C, Tonon G, Richardson PG, Anderson KC. Understanding multiple myeloma pathogenesis in the bone marrow to identify new therapeutic targets. Nat Rev Cancer. 2007; 7(8):585–98. [PubMed: 17646864]

28. Tai YT, Podar K, Catley L, Tseng YH, Akiyama M, Shringarpure R, et al. Insulin-like growth factor-1 induces adhesion and migration in human multiple myeloma cells via activation of beta1-integrin and phosphatidylinositol 3'-kinase/AKT signaling. Cancer Res. 2003; 63(18):5850–8. [PubMed: 14522909]

29. Chauhan D, Li G, Shringarpure R, Podar K, Ohtake Y, Hideshima T, et al. Blockade of Hsp27 overcomes Bortezomib/proteasome inhibitor PS-341 resistance in lymphoma cells. Cancer Res. 2003; 63(19):6174–7. [PubMed: 14559800]

30. Hideshima T, Podar K, Chauhan D, Ishitsuka K, Mitsiades C, Tai YT, et al. p38 MAPK inhibition enhances PS-341 (bortezomib)-induced cytotoxicity against multiple myeloma cells. Oncogene. 2004; 23(54):8766–76. [PubMed: 15480425]

31. Yasui H, Hideshima T, Ikeda H, Jin J, Ocio EM, Kiziltepe T, et al. BIRB 796 enhances cytotoxicity triggered by bortezomib, heat shock protein (Hsp) 90 inhibitor, and dexamethasone via inhibition of p38 mitogen-activated protein kinase/Hsp27 pathway in multiple myeloma cell lines and inhibits paracrine tumour growth. Br J Haematol. 2007; 136(3):414–23. [PubMed: 17173546]

32. Ishitsuka K, Hideshima T, Neri P, Vallet S, Shiraishi N, Okawa Y, et al. p38 mitogen-activated protein kinase inhibitor LY2228820 enhances bortezomib-induced cytotoxicity and inhibits osteoclastogenesis in multiple myeloma; therapeutic implications. Br J Haematol. 2008; 141(5): 598–606. [PubMed: 18397345]

33. Matsumoto M, Sudo T, Saito T, Osada H, Tsujimoto M. Involvement of p38 mitogen-activated protein kinase signaling pathway in osteoclastogenesis mediated by receptor activator of NF-kappa B ligand (RANKL). J Biol Chem. 2000; 275(40):31155–61. [PubMed: 10859303]

34. Abe M, Hiura K, Wilde J, Shioyasono A, Moriyama K, Hashimoto T, et al. Osteoclasts enhance myeloma cell growth and survival via cell-cell contact: a vicious cycle between bone destruction and myeloma expansion. Blood. 2004; 104(8):2484–91. [PubMed: 15187021]

35. Ouk S, Liou ML, Liou HC. Direct Rel/NF-kappaB inhibitors: structural basis for mechanism of action. Future Med Chem. 2009; 1(9):1683–707. [PubMed: 21425986]

36. Oerlemans R, Franke NE, Assaraf YG, Cloos J, van Zantwijk I, Berkers CR, et al. Molecular basis of bortezomib resistance: proteasome subunit beta5 (PSMB5) gene mutation and overexpression of PSMB5 protein. Blood. 2008; 112(6):2489–99. [PubMed: 18565852]

37. Ri M, Iida S, Nakashima T, Miyazaki H, Mori F, Ito A, et al. Bortezomib-resistant myeloma cell lines: a role for mutated PSMB5 in preventing the accumulation of unfolded proteins and fatal ER stress. Leukemia. 2010; 24(8):1506–12. [PubMed: 20555361]

38. McConkey DJ, Zhu K. Mechanisms of proteasome inhibitor action and resistance in cancer. Drug Resist Updat. 2008; 11(4–5):164–79. [PubMed: 18818117]

39. Anderson KC. Targeted therapy of multiple myeloma based upon tumor-microenvironmental interactions. Exp Hematol. 2007; 35(4 Suppl 1):155–62. [PubMed: 17379101]

40. Markovina S, Callander NS, O'Connor SL, Kim J, Werndli JE, Raschko M, et al. Bortezomib-resistant nuclear factor-kappaB activity in multiple myeloma cells. Mol Cancer Res. 2008; 6(8): 1356–64. [PubMed: 18708367]

41. Markovina S, Callander NS, O'Connor SL, Xu G, Shi Y, Leith CP, et al. Bone marrow stromal cells from multiple myeloma patients uniquely induce bortezomib resistant NF-kappaB activity in myeloma cells. Mol Cancer. 2010; 9:176. [PubMed: 20604947]

42. Xiao W, Hodge DR, Wang L, Yang X, Zhang X, Farrar WL. NF-kappaB activates IL-6 expression through cooperation with c-Jun and IL6-AP1 site, but is independent of its IL6-NFkappaB regulatory site in autocrine human multiple myeloma cells. Cancer Biol Ther. 2004; 3(10):1007–17. [PubMed: 15467434]

43. Xiao W, Hodge DR, Wang L, Yang X, Zhang X, Farrar WL. Co-operative functions between nuclear factors NFkappaB and CCAT/enhancer-binding protein-beta (C/EBP-beta) regulate the IL-6 promoter in autocrine human prostate cancer cells. Prostate. 2004; 61(4):354–70. [PubMed: 15389813]

44. Franzoso G, Carlson L, Xing L, Poljak L, Shores EW, Brown KD, et al. Requirement for NF-kappaB in osteoclast and B-cell development. Genes Dev. 1997; 11(24):3482–96. [PubMed: 9407039]

45. Zheng H, Yu X, Collin-Osdoby P, Osdoby P. RANKL stimulates inducible nitric-oxide synthase expression and nitric oxide production in developing osteoclasts. An autocrine negative feedback mechanism triggered by RANKL-induced interferon-beta via NF-kappaB that restrains osteoclastogenesis and bone resorption. J Biol Chem. 2006; 281(23):15809–20. [PubMed: 16613848]

46. Iotsova V, Caamano J, Loy J, Yang Y, Lewin A, Bravo R. Osteopetrosis in mice lacking NF-kappaB1 and NF-kappaB2. Nat Med. 1997; 3(11):1285–9. [PubMed: 9359707]

47. Xing L, Carlson L, Story B, Tai Z, Keng P, Siebenlist U, et al. Expression of either NF-kappaB p50 or p52 in osteoclast precursors is required for IL-1-induced bone resorption. J Bone Miner Res. 2003; 18(2):260–9. [PubMed: 12568403]

48. Yamamoto A, Miyazaki T, Kadono Y, Takayanagi H, Miura T, Nishina H, et al. Possible involvement of IkappaB kinase 2 and MKK7 in osteoclastogenesis induced by receptor activator of nuclear factor kappaB ligand. J Bone Miner Res. 2002; 17(4):612–21. [PubMed: 11918218]

49. von Metzler I, Krebbel H, Hecht M, Manz RA, Fleissner C, Mieth M, et al. Bortezomib inhibits human osteoclastogenesis. Leukemia. 2007; 21(9):2025–34. [PubMed: 17581612]

50. Hongming H, Jian H. Bortezomib inhibits maturation and function of osteoclasts from PBMCs of patients with multiple myeloma by downregulating TRAF6. Leuk Res. 2009; 33(1):115–22. [PubMed: 18778854]

Translational relevance

NF-κB transcription factor plays a key role in the pathogenesis of multiple myeloma (MM) in the context of the bone marrow (BM) microenvironment. Several studies validate NF-κB pathway as a promising therapeutic target in MM, with both canonical and non-canonical pathways contributing to total NF-κB activity. However, selective inhibitors against these pathways have not yet been developed. The preclinical study presented here is designed to characterize the anti-tumor activity of PBS-1086, a dual inhibitor of NF-κB pathways, *in vitro* in MM cell lines, patient MM cells, and also in the presence of BMSCs. We demonstrate that PBS-1086 induces potent selective cytotoxicity in MM cells and overcomes the prosurvival advantage conferred by the BM milieu. We show a synergistic cytotoxicity in bortezomib-resistant MM cell lines and patient MM cells, suggesting a potential clinical use of PBS-1086 in combination with bortezomib. In addition, our results indicate that PBS-1086 inhibits osteoclast activity, suggesting potential benefit in MM-related bone disease. Finally, PBS-1086 demonstrates significant anti-tumor activity in a human MM xenograft murine model with improvement of overall survival. Our preclinical study provides the rationale for clinical evaluation of PBS-1086 in combination with bortezomib for the treatment of MM.

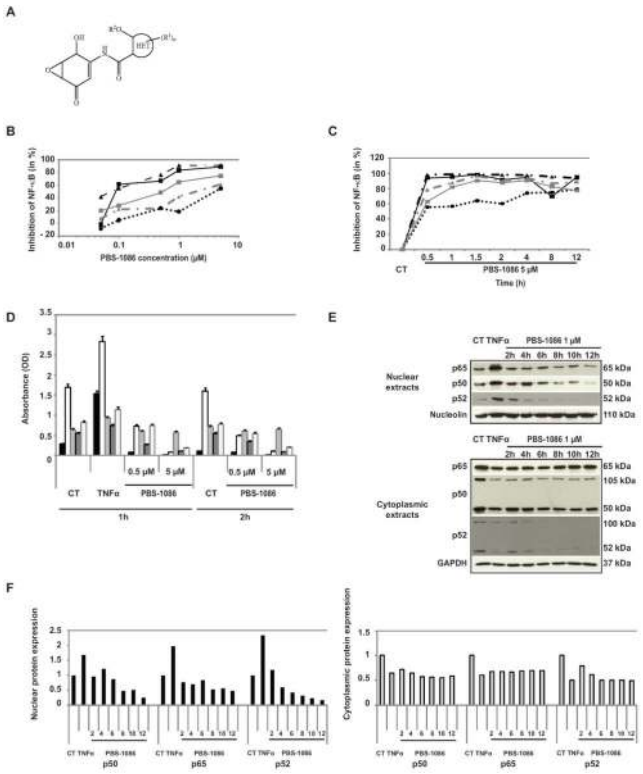

Figure 1. PBS-1086 inhibits both canonical and non-canonical NF-κB pathways

(A) Chemical structure of PBS-1086.

(B) MM.1S cells were cultured with PBS-1086 at the indicated doses (0.01, 0.1, 1 and 10 μM) for 2 hours. NF-κB DNA binding activity in MM.1S nuclear extracts was assessed *in vitro* using Trans-AM NF-κB Family Transcription Factor Assay Kit. NF-κB canonical activity included p65 (—■—), p50 (--▲--), and c-Rel (--●--); NF-κB non-canonical activity included p52 (—■—) and RelB (--▲--). **(C)** MM.1S cells were cultured with PBS-1086 (5 μM) at the indicated times (0.5 to 12 hours). NF-κB DNA binding activity in MM.1S nuclear extracts was measured by ELISA. NF-κB canonical activity included p65 (—■—), p50 (--▲--), and c-Rel (--●--); NF-κB non-canonical activity included p52 (—■—) and RelB (--▲--). Results are expressed as percent inhibition from the quantity of NF-κB protein bound in the PBS-1086 treated relative to the maximum quantity bound in the control. ELISA data shown are representative of three independent experiments.

(D) MM.1S cells were treated with PBS-1086 (0.5 and 5 μM) for the indicated times (1 and 2 hours). NF-κB DNA binding activity in MM.1S nuclear extracts was measured by ELISA. NF-κB canonical activity included p65 (■), p50 (□), and c-Rel (■); NF-κB non-canonical activity included p52 (■) and RelB (□). Treatment with TNF-α (10 ng/ml) for 1 hour served as a positive control of NF-κB activity for both time points, 1 and 2 hours. The results of ELISA are expressed as relative absorbance. Data represent mean +/− SD of three independent experiments.

(E) MM.1S cells were cultured with PBS-1086 (1 μM) for the indicated times (2 to 12 hours). Treatment with TNF-α (10 ng/ml) for 1 hour served as a positive control of increased p65, p50, and p52 nuclear translocation. Nuclear and cytoplasmic extracts were subjected to Western blotting using p50, p52, p65, GAPDH, and Nucleolin antibodies.

GAPDH and Nucleolin were used as purity and loading controls for cytoplasmic and nuclear extracts, respectively. Blots are representative of three independent experiments.
(F) The densitometric analysis of scanned immunoblotting images was performed with the NIH image J Software. Results of nuclear (■) (left panel) and cytoplasmic (□) (right panel) protein expression are expressed as fold change relative to control.

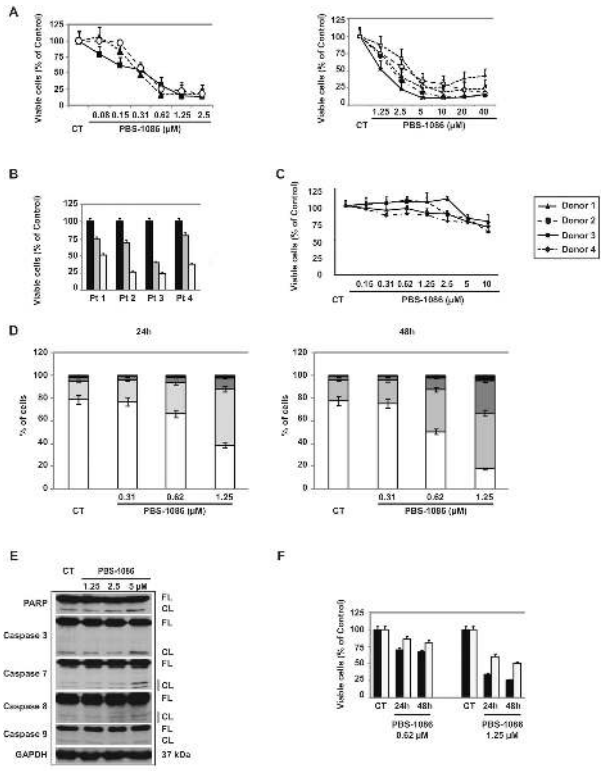

Figure 2. PBS-1086 induces cytotoxicity and apoptosis in MM cells

(A) MM cell lines MM.1S (—■—), INA6 (--▲--), and KMS18 (– O –) were cultured with PBS-1086 (0.08–2.5 μM) for 48 hours (left panel). MM cell lines MM.1R (—✱—), Dox40 (--◆--), LR5 (– O –), RPMI 8226 (– ● –), and U266 (--◇--) were treated with PBS-1086 (1.25–40 μM) for 48 hours (right panel). **(B)** CD138+ MM cells from four patients were treated with PBS-1086 0 (■), 0.62 (▣) and 1.25 μM (□) for 48 hours. **(C)** Mononuclear cells isolated from four healthy donors and stimulated by phytohemagglutinin were cultured with PBS-1086 (0.15–10 μM) for 48 hours. Cell viability was assessed by MTT assay of triplicate cultures, expressed as percentage of untreated control. Data represent mean +/− SD viability.

(D) MM.1S cells were treated with PBS-1086 at the indicated doses (0.31 to 1.25 μM) for 24 and 48 hours. Apoptotic cells were analyzed by flow cytometry using Annexin V/PI staining. Percentages of viable (AV−/PI−) (□), early apoptotic (AV+/PI−) (▣), late apoptotic (AV+/PI+) (▣) and necrotic cells (AV−/PI+) (■) are shown as a histogram. Data represent mean +/− SD of three independent experiments.

(E) MM.1S cells were cultured with PBS-1086 at the indicated doses (1.25 to 5 μM) for 24 hours. Whole cell lysates were subjected to Western blotting using anti-caspase 3, caspase 7, caspase 8, caspase 9, PARP and GAPDH antibodies. FL indicates full length, and CF denotes cleaved fragment. GAPDH was used as a loading control. Blots are representative of three independent experiments.

(F) MM.1S cells were cultured with PBS-1086 (0.62 and 1.25 μM) for 24 and 48 hours in the presence (□) or absence (■) of z-VAD (20 μM). Cell viability was assessed by MTT assay of triplicate cultures, expressed as percentage of untreated control. Data represent mean +/− SD viability.

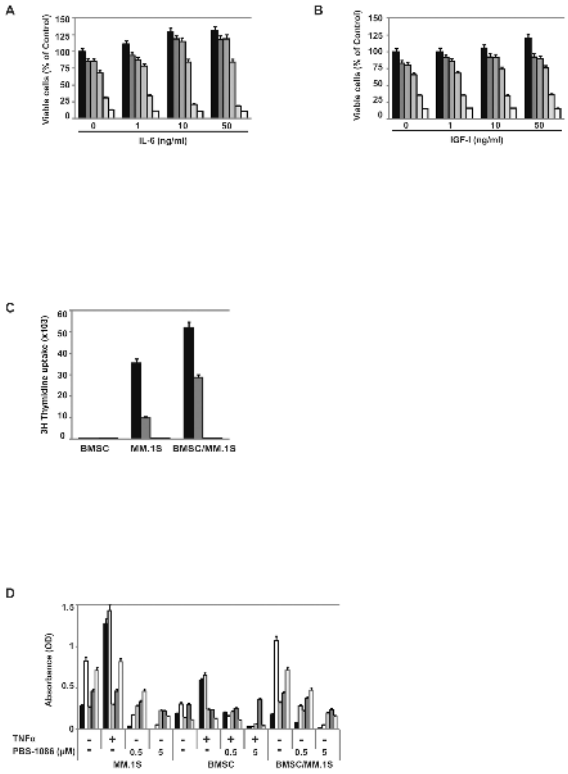

Figure 3. PBS-1086 overcomes the proliferative and anti-apoptotic effects of BMSCs associated with inhibition of NF-κB

(A) MM.1S cells were cultured for 48 hours with PBS-1086 0 (■), 0.15 (■), 0.31 (■), 0.62 (■), 1.25 (□), and 2.5 μM (□), in the absence or presence of IL-6 (1, 10 and 50 ng/ml). **(B)** MM.1S cells were cultured for 48 hours with PBS-1086 0 (■), 0.15 (■), 0.31 (■), 0.62 (■), 1.25 (□), and 2.5 μM (□), in the absence or presence of IGF-I (1, 10 and 50 ng/ml). Cell viability was assessed by MTT assay of triplicate cultures, expressed as percentage of untreated control. Data represent mean +/− SD viability.

(C) MM.1S cells were treated for 48 hours with PBS-1086 0 (■), 0.62 (■), 1.25 (■), and 2.5 μM (■), in the presence or absence of BMSCs. Cell viability was assessed by thymidine uptake of quadruplicate cultures, expressed as percentage of untreated control. Data represent mean +/− SD viability.

(D) MM.1S cells were treated for 2 hours with PBS-1086 (0.5 and 5 μM), in the presence or absence of BMSCs. NF-κB DNA binding activity in MM.1S +/− BMSCs nuclear extracts was measured by ELISA. NF-κB canonical activity included p65 (■), p50 (□), c-Rel (■); NF-κB non-canonical activity included p52 (■) and RelB (□). Treatment with TNF-α (10 ng/ml) for 2 hours served as a positive control of NF-κB activation in MM.1S cells. The results of ELISA were expressed as relative absorbance. Data represent mean +/− SD of three independent experiments.

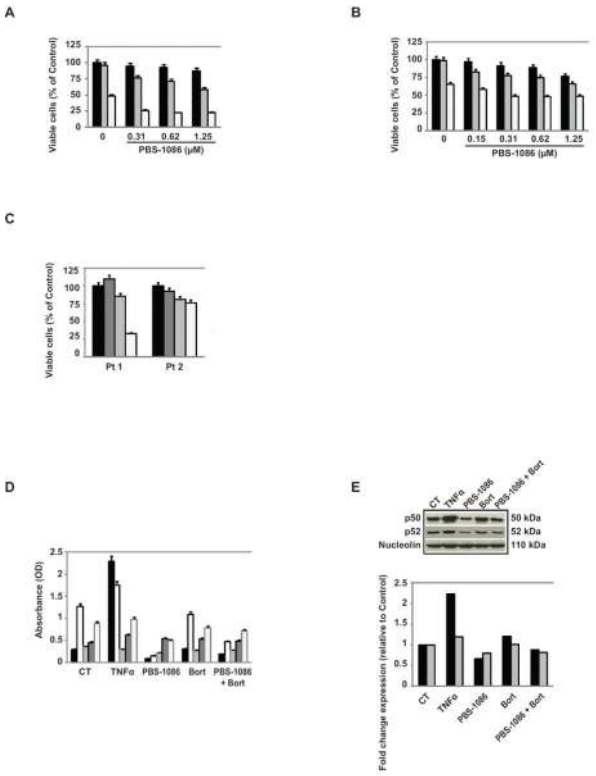

Figure 4. PBS-1086 enhances MM cytotoxicity of bortezomib in bortezomib-resistant MM cells

(A) Dox40 cells were cultured for 72 hours with bortezomib (Bort) 0 (■), 10 (■) and 15 nM (■), in the presence or absence of PBS-1086 (0.31–1.25 μM). **(B)** ANBL6-VR5 cells were cultured for 48 hours with bortezomib (Bort) 0 (■), 10 (■) and 20 nM (■), in the presence or absence of PBS-1086 (0.15–1.25 μM). Cell viability was assessed by MTT assay of triplicate cultures, expressed as percentage of untreated control. Data represent mean +/− SD viability.

(C) CD138+ MM cells from two patients with bortezomib-resistant MM (Pt1 and Pt2) were treated with bortezomib (Bort) 10 nM (■) alone, PBS-1086 (1.25 μM) (■) alone, PBS-1086+Bort (■), or not treated (■) for 48 hours. Cell viability was assessed by MTT assay of triplicate cultures, expressed as percentage of untreated control. Data represent mean +/− SD viability.

(D) ANBL6-VR5 cells were treated for 2 hours with PBS-1086 (1 μM), in the presence or absence of bortezomib (40 nM). NF-κB canonical activity included p65 (■), p50 (■), c-Rel (■); NF-κB non-canonical activity included p52 (■) and RelB (■). Treatment with TNF-α (10 ng/ml) for 2 hours served as a positive control of NF-κB activation in ANBL6-VR5 cells. The results of ELISA were expressed as relative absorbance. Data represent mean +/− SD of three independent experiments.

(E) Corresponding nuclear extracts from ANBL6-VR5 cells treated for 2 hours with PBS-1086 (1 μM) +/− bortezomib (40 nM) were subjected to Western blotting using p50, p52, and Nucleolin antibodies. Blots are representative of three independent experiments. The densitometric analysis of scanned immunoblotting images for p50 (■) and p52 (■) was performed with the NIH image J Software and expressed as fold change relative to non-treated cells.

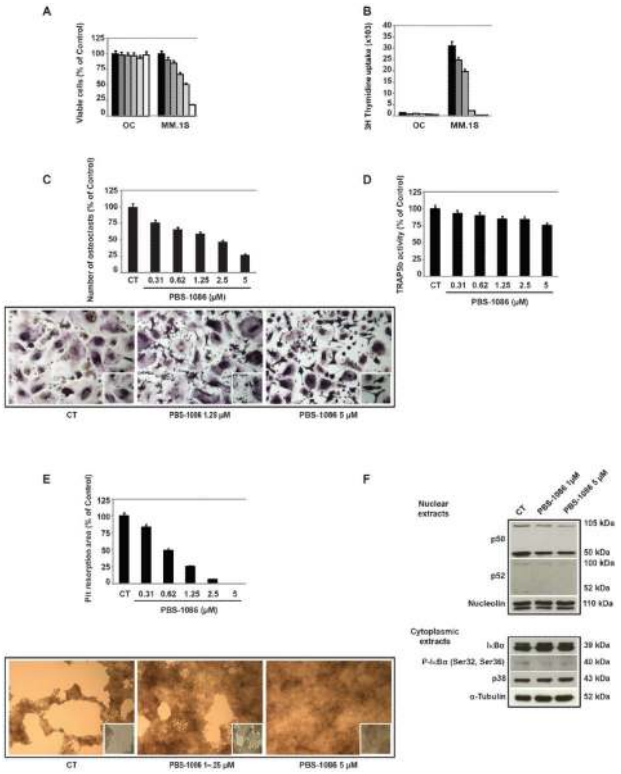

Figure 5. PBS-1086 inhibits osteoclast activity associated with inhibition of NF-κkB

(A) Osteoclasts (OC) and MM.1S cells were cultured for 48 hours with PBS-1086 0 (■), 0.31 (■), 0.62 (■), 1.25 (■), 2.5 (■), and 5 μM (■). Cell viability was assessed by MTT assay of triplicate cultures, expressed as percentage of untreated control. Data represent mean +/− SD viability. **(B)** Cell viability was assessed by thymidine uptake of quadruplicate cultures, expressed as percentage of untreated control. Data represent mean +/− SD viability. **(C)** Mature osteoclasts (OC) were treated for 48 hours with PBS-1086 (0.31-5 μM). Cells were stained for TRAP activity. Cell density was equal in all samples. TRAP positive multinucleated osteoclasts after PBS-1086 treatment are quantitated as percentage of untreated control. For non-treated control as well as PBS-1086 1.25 and 5 μM treated cultures, the corresponding micrographs are shown (10×), with inserts at higher magnification. Data represent mean +/− SD counts of three independent experiments. **(D)** Mature osteoclasts (OC) were treated for 48 hours with PBS-1086 (0.31-5 μM). The presence of TRAP5b in the supernatants of culture was quantified by ELISA, expressed as percentage of untreated control. Data represent mean +/− SD absorbance of triplicate experiments.

(E) Primary human osteoclast precursors derived from two MM patients were seeded on calcium phosphate-coated plates. Cells were treated with PBS-1086 (0.31-5 μM) in the presence of M-CSF (25 ng/ml) and RANKL (50 ng/ml) to mature osteoclasts. Osteoclasts not stimulated with M-SCF nor RANKL served as a negative control and failed to resorb. Osteoclasts stimulated with M-CSF and RANKL (positive control) resorbed calcium phosphate (>95%). The average pit resorption area with PBS-1086 was expressed as percentage of positive control. For non-treated control, as well as PBS-1086 1.25 and 5 μM

treated cultures, the corresponding micrographs are shown (10×), with inserts at higher magnification. Data represent mean +/− SD of four independent experiments.
(F) Nuclear and cytoplasmic extracts from mature osteoclasts were cultured for 2 hours with PBS-1086 at 1 and 5 μM. Control non-treated osteoclasts were only stimulated with RANKL and M-CSF. Nuclear extracts were subjected to Western blotting using p50, p52, and Nucleolin antibodies. Cytoplasmic extracts were subjected to Western blotting using IκBα, P-IκBα (Ser 32/36), p38, and α-Tubulin antibodies. Nucleolin and α-Tubulin were used as purity and loading controls for nuclear and cytoplasmic extracts, respectively. Blots are representative of three independent experiments.

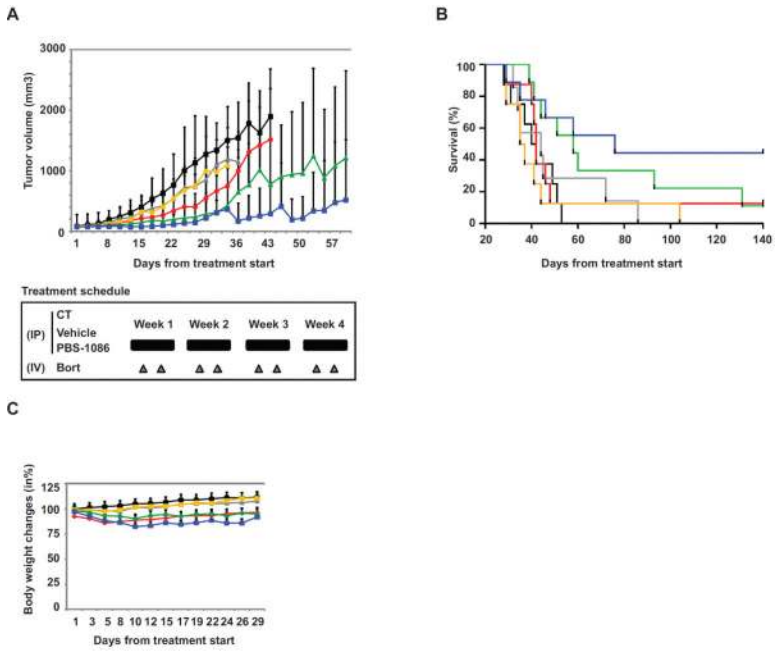

Figure 6. PBS-1086 inhibits tumor growth in a murine xenograft model of human MM

(A) SCID mice were injected subcutaneously with 5×10^6 MM.1S cells and treated with 7.5 mg/kg PBS-1086 IP daily for 4 weeks (—) (n=8); 0.5 mg/kg bortezomib IV twice a week for 4 weeks (—) (n=8); PBS-1086 at 2.5 mg/kg IP and bortezomib IV (—) (n=9); or PBS-1086 at 7.5 mg/kg IP and bortezomib IV (—) (n=9). A vehicle control group (—) (n=8) received IP injections of vehicle alone daily for 4 weeks. The non-treated control (CT) group (—) (n=8) received IP injections of saline daily for 4 weeks. Tumor volume was calculated from caliper measurements three times per week, and error bars represent +/− SE. Tumor volume curve extends to 57 days from the first day of treatment, when half of the mice per group have died.

(B) Survival was evaluated from the first day of treatment using Kaplan-Meier curves.

(C) Body weight of mice treated with PBS-1086, bortezomib (Bort), PBS-1086+bortezomib (PBS-1086+Bort), vehicle (Veh) or control (CT) was expressed as percentage of baseline. Body weight curve extends to 29 days from the first day of treatment, when the death in any of the groups was first observed. Error bars represent +/− SD body weight.